

Queue-Aware Optimal Frequency Selection for Energy Minimization in Wireless Networks

Jie Chen and Biplab Sikdar

Department of ECSE, Rensselaer Polytechnic Institute, Troy, NY, 12180

Department of ECE, National University of Singapore, Singapore

Abstract—Reducing the energy consumption of wireless networks is one of the fundamental objectives of green networks. While the use of dynamic frequency scaling has been proposed for reducing the energy consumption, they increase the packet delays and loss rates in the network. This paper addresses the problem of optimally selecting the clock frequency for wireless network interface cards with dynamic frequency scaling, so that the energy consumption is minimized while meeting the packet level performance requirements. The proposed framework is based on modeling the interface card as a $MAP/G/1/K$ with threshold based service. The proposed frequency selection mechanism has been verified through simulations.

I. INTRODUCTION

Green communication networks that are designed with the objective of reducing the energy consumption and environmental impact of information and communication technologies (ICT) are gaining popularity. Among the various possibilities for reducing the energy consumption, the development of energy efficient protocols at various layers has been the most common avenue of research. However, these protocols run on traditional networking hardware that are generally agnostic of the load and whose energy consumption is not load-proportional. Thus these devices consume close to the maximum energy rating even when the load is low [1], [2].

To provide load proportional energy usage, the use of hardware equipped with dynamic voltage and frequency scaling (DVFS) has been proposed in literature [3], [4]. DVFS techniques reduce the energy consumption by reducing the supply voltage and/or the clock frequency to the circuits. However, the reduction in the energy consumption is accompanied by an increase in the packet processing times, thereby leading to larger queue lengths and packet delays, and the possibility of packet loss. Thus there is a direct relation between the energy savings and the likelihood of queue instability and the selection of the clock frequency plays a critical role in achieving the tradeoff between the energy consumption and packet delays. This paper addresses the problem of optimal frequency selection in dynamic frequency scaling (DFS) systems for wireless networks that minimizes the energy consumption while ensuring that constraints on the packet level delay and loss rates are met.

To address the problem of optimal frequency selection at a wireless device, this paper develops a threshold-based frequency selection mechanism where the selection is based on observations of the device's queue length. To design the

frequency selection mechanism, we first develop an analytic model to quantify the relationship between the energy savings and the dynamics of the queues at the devices. We model each wireless node as a $MAP/G/1/K$ queue where the service time distribution depends on the instantaneous queue length when a packet begins service. This modeling framework is then used to evaluate the tradeoff between the energy savings and packet level delay and loss performance in order to set the optimal thresholds on the queue length for frequency selection. The proposed frequency selection mechanism has been evaluated and validated using simulations conducted on the NS-2 simulation platform.

The rest of the paper is organized as follows. In Section II we describe the system model assumed in this paper. Section III presents the proposed queueing model for quantifying the packet delays and losses associated with any threshold-based frequency selection strategy. Section IV presents the methodology for determining the optimal frequency thresholds. Section V presents the simulation results to evaluate the proposed framework. Finally, Section VI concludes the paper.

II. SYSTEM MODEL

The focus of this paper is on general wireless local area networks. The access to wireless networks at any node is usually through the use of a network interface card, the fundamental building blocks of which are shown in Figure 1. Consequently, the system model does not assume any particular medium access control (MAC) protocol. As shown in Figure 1, a generic wireless network interface card typically consists of the following functional blocks: blocks for radio frequency (RF) transmit and receive operations, blocks that implement the MAC and physical (PHY) layers for the wireless network, transmit (TX) and receive (RX) buffers that are controlled by a buffer manager, optional units for management and Internet Protocol Security (IPSec), and a control unit. Finally, the network card is connected to the host node either through a communication block (e.g. Peripheral Component Interconnect (PCI) bus) or, in the case of an wireless access point, PHY and MAC layers for the wired network interface (e.g. Ethernet).

In contrast to traditional systems where the supply voltage and clock frequencies of the functional blocks are kept constant at all times, systems with DVFS vary the voltage and clock rates of some or all of the functional blocks in order to save energy. The energy savings with DVFS comes from the fact that the energy consumption of electronic devices

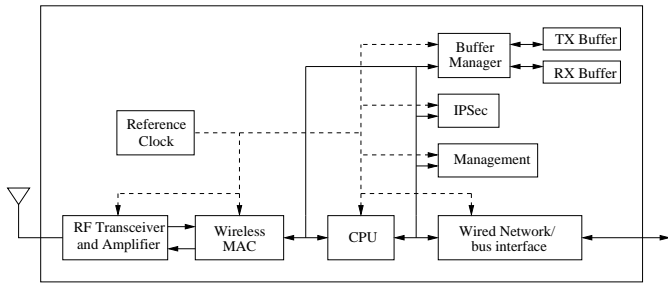


Fig. 1. Simplified block diagram of a wireless network interface.

is dependent on three factors: the operating voltage and frequency, and the effective capacitance of the device. The energy consumption of a device can be written as [5]:

$$P = \alpha C_{eff} V^2 f \quad (1)$$

where α is the switching factor, C_{eff} is the effective capacitance, V denotes the operating voltage and f is the operating frequency. Since the energy consumption is related to both the voltage and the clock frequency, either may be varied to achieve energy savings. However, practical implementation of voltage scaling is challenging and associated with considerable overhead [3]. Consequently, this paper focuses on the use of DFS. In this paper, as in [5], we further assume that

$$V^2 \propto f. \quad (2)$$

Hence,

$$P \propto f^2. \quad (3)$$

III. QUEUEING MODEL FOR ENERGY-PERFORMANCE TRADEOFF

A fundamental aspect of the use of DFS is that the energy savings comes with a cost on the performance. As the clock frequency is reduced, the rate at which packets are processed is also reduced, increasing the packet delays and loss rates. Consequently, the selection of the operating frequency should be made such that the energy savings are balanced with the other aspects of system performance.

DFS mechanisms such as those proposed in [4], [6] are based on selecting the operating frequency by observing the queue levels at the nodes. This paper assumes a similar approach. Let the maximum buffer size of the transmit queue at a node be denoted by B . Also, consider a DFS mechanism implemented in the network interface card that provides a set of N operating frequencies, \mathcal{F} , with $|\mathcal{F}| = N$, to choose from. Let $f_1 < f_2 < \dots < f_N$ and let P_i denote the the rate of energy consumption of the network interface card when frequency f_i , $1 \leq i \leq N$, is selected. From Equation (3), we then have $P_1 < P_2 < \dots < P_N$. To select the operating frequency, a threshold based policy is used. The transmit buffer of size B is demarcated into N regions using the threshold values L_1, L_2, \dots, L_{N-1} . Also, we define $L_0 = 1$ and $L_N = B$. Then, operating frequency f_i is chosen, $1 \leq i \leq N$ if the current queue length of the TX buffer Q satisfies $L_{i-1} \leq Q < L_i$, for $1 \leq i \leq N - 1$, and frequency f_N is chosen if $Q > L_{N-1}$.

The packet level performance of the network interface card as well as the energy savings depend on the choice of the thresholds, L_i , $1 \leq i \leq N - 1$. To characterize this relationship, we develop a queueing model for each node. To accommodate a wide range of arrival process such as voice, data, video as well as long-range dependent traffic, we model the arrival process at each node as a generalized Markovian arrival process (MAP) [7], [8]. We consider a $m + 1$ state, continuous-time Markov process where the states $1, \dots, m$ are transient and state $m + 1$ is absorbing. In state i , $1 \leq i \leq m$, the sojourn time is exponentially distributed with parameter λ_i . The probability that the process enters the absorbing state from state i and immediately restarts in state j with $1 \leq i, j, \leq m$ is denoted by $p_{i,j}$. Similarly, $q_{i,j}$ denotes the probability that the process enters state j from state i without being absorbed, with $1 \leq i, j, \leq m$ and $i \neq j$. The evolution of the arrival process is defined by the $m \times m$ matrices C and D whose elements are given by

$$\begin{aligned} C_{i,j} &= \lambda_i q_{i,j} & i \neq j \\ C_{i,i} &= -\lambda_i \\ D_{i,j} &= \lambda_i p_{i,j} & 1 \leq i, j, \leq m \end{aligned} \quad (4)$$

We assume that the matrix C is non-singular and the steady-state probability vectors of the Markov process π is given by the solution of the equations

$$\pi(C + D) = 0, \quad \pi e = 1 \quad (5)$$

where e is an unit column vector. The mean arrival rate of the MAP is given by

$$\bar{\lambda} = \pi D e. \quad (6)$$

The service time of a packet depends on three factors: the selected clock frequency which determines the rate at which the packet is processed (e.g. framing, encryption, cyclic redundancy check etc.), the channel contention time, and the packet length which determines the transmission time. The channel contention and transmission times are independent of the clock frequency selected through DFS. We denote the probability distribution function (pdf) of the channel contention time by $g_r(x)$. Note that the contention time for protocols such as IEEE 802.11 are well known [9]. We also denote the pdf of the transmission time by $g_t(x)$, where the transmission time includes the time required for the transmission of control packets such as the acknowledgment. Finally, given that the selected clock frequency is f_i , the pdf of the service time required for packet processing is denoted by $g_{p,i}(x)$. We denote the pdf of the overall service time and its expected value when frequency f_i , $1 \leq i \leq N$, is selected by $g_{S,i}(x)$ and s_i , respectively. The Laplace-Stieltjes transform of this service time is given by

$$G_i(s) = R(s)T(s)P_i(s) \quad (7)$$

where $R(s)$, $T(s)$, and $P_i(s)$ are the Laplace-Stieltjes transforms of $g_r(x)$, $g_t(x)$ and $g_{p,i}(x)$, respectively.

Our system corresponds to a queue with arrivals characterized by a MAP, general service times characterized in Eqn. (7),

a single server, and a finite buffer of size B . However, unlike traditional queueing systems, the service time distribution of each packet is not identical, but depends on the queue length at the time the service is initiated. To analyze this $MAP/G/1/B$ queue with service time based on queue lengths, we use the model from [10]. We first characterize the stationary queue length distribution at an arbitrary time t . Let $Q(t)$ and $J(t)$ denote the number of packets in the queue and the state of the Markov arrival process, respectively, at time t . Also, let $\chi(t)$ be a random variable that takes the value i if the selected frequency at time t is f_i , with $1 \leq i \leq N$. Also, let $\xi(t)$ be a binary valued random variable that takes a value of 0 if the server is idle at time t , and a value of 1 otherwise. The steady state probabilities of the queue length are defined as

$$\begin{aligned} y(0, j) &= \lim_{t \rightarrow \infty} Pr\{Q(t) = 0, J(t) = j, \xi(t) = 0\} \\ y_0 &= (y(0, 1), y(0, 2), \dots, y(0, m)) \\ y^r(n, j) &= \lim_{t \rightarrow \infty} Pr\{Q(t) = n, J(t) = j, \chi(t) = r, \xi(t) = i\} \\ y_n^r &= (y^r(n, 1), y^r(n, 2), \dots, y^r(n, m)) \\ y_n &= \sum_{r=1}^{N-1} y_n^r, \quad 1 \leq n \leq B \end{aligned}$$

for $1 \leq j \leq m$ and $r = 1, \dots, N-1$. In [10], it has been shown that the stationary probability distribution of the queue occupancy, y , is given by

$$y_0 = \frac{1}{E} x_0 (-C^{-1}) \quad (8)$$

$$y_B = \pi - \sum_{k=0}^{B-1} y_k \quad (9)$$

and for $1 \leq n < B$,

$$\begin{aligned} y_n &= \frac{1}{E} \left[x_0 (-C^{-1}) D \sum_{l=0}^{n-1} A_l^1 C^{-1} [D(-C^{-1})]^{n-l-1} \right. \\ &\quad + \sum_{r=1}^N \sum_{k=L_{r-1}}^{\min\{n, L_r-1\}} x_k \sum_{l=0}^{n-k} A_l^r C^{-1} [D(-C^{-1})]^{n-l-k} \\ &\quad \left. - \sum_{k=0}^n x_k C^{-1} [D(-C^{-1})]^{n-k} \right] \quad (10) \end{aligned}$$

where $\sum_{k=a}^b x_k = 0$ if $b < a$, and the parameters E , x and A are defined in the Appendix.

The average energy consumed by the node is then given by

$$\varepsilon = \sum_{r=1}^N \sum_{i=L_{r-1}}^{L_r-1} P_k y_i e + P_N y_B e + P_1 y_0 e \quad (11)$$

The packet loss probability, P_{loss} , and the average packet delay, W , are given by

$$P_{loss} = \frac{y_B D e}{\sum_{i=0}^B y_i D e} \quad (12)$$

$$W = \frac{\sum_{i=0}^B i y_i e}{\lambda(1 - P_{loss})}. \quad (13)$$

Algorithm 1 Threshold Selection Process

```

1: Input:  $B, N, \rho, \omega, f_i, P_i \ 1 \leq i \leq N$ ;
2: Initialize:  $L_N = B, L_0 = 1$ ;
3: Initialize:  $S = \{L_0, L_N\}$ ;
4: Initialize:  $\mathcal{F} = \{f_N\}$ ;
5: FEASIBILITY CHECK
6: if  $(P_{loss}, W)_{MAP/G/1/B(S, \mathcal{F})} > (\rho, \omega)$  then
7:   Exit: Solution not feasible;
8: end if
9: THRESHOLD DETERMINATION
10: for  $i = N-1$  to 1 by 1 do
11:   Initialize:  $L_i = L_0$ ;
12:    $S = S \cup L_i$ ;
13:    $\mathcal{F} = \mathcal{F} \cup f_i$ ;
14:    $L_i = \arg \max_{L_i \in (L_0, L_{i+1})} [(P_{loss}, W)_{MAP/G/1/B(S, \mathcal{F})} \leq (\rho, \omega)]$ ;
15: end for

```

IV. SELECTION OF OPTIMAL THRESHOLDS

The previous section provides a model that captures the relationship between the frequency selected with performance metrics of interest such as the energy consumption, packet delays and the packet loss rates. This section uses this framework to obtain the optimal thresholds for frequency selection.

We consider a scenario where the traffic characteristics of the arrival process, in terms of the matrices C and D are known. Then, the objective of the DFS mechanism is to select the operating frequency such that the overall energy consumption at a node is minimized, while satisfying average packet delay and loss requirements. This optimization problem may be written as:

$$\begin{aligned} \mathbf{P1:} \quad & \min_{L_k} \sum_{r=1}^N \sum_{i=L_{r-1}}^{L_r-1} P_k y_i e + P_N y_B e + P_1 y_0 e \\ & \text{subject to } P_{loss} \leq \rho \\ & W \leq \omega \end{aligned}$$

where ρ and ω are the maximum allowable limits on the average loss rates and delay, respectively. Note that variations of the optimization problem **P1** may include cases where the constraint is only on the packet loss or the packet delays.

It is obvious that problem **P1** is complex and a closed form solution for the optimal threshold levels does not exist. To solve the problem with reasonable complexity, we propose a heuristic as shown in Algorithm 1. Algorithm 1 is a greedy approach for selecting the queue thresholds for frequency selection. We first start with a system with only one available clock frequency: f_N . The first step is to check if the target loss and delay requirements can be met. We start by obtaining the values of the delay and loss as obtained from the results for Section III for the system with only the highest clock frequency (denoted in Algorithm 1 by $(P_{loss}, W)_{MAP/G/1/B(S, \mathcal{F})}$), and checking against the specified loss and delay constraints. If the desired targets cannot be achieved when only the highest frequency is used,

then it is obvious that using lower frequencies would still result in an infeasible solution.

For a system that passes the feasibility check, we set the threshold for each frequency, starting with the highest. For the i -th frequency, we thus consider a system with the highest i frequencies (the set \mathcal{F}) and for which the threshold for the frequencies f_{i+1}, \dots, f_N have already been determined (the set \mathcal{S}). For this system, we then choose the threshold for the i -th frequency between the lowest threshold possible (L_0) and the queue threshold for the next highest frequency (L_{i+1}). In this range, we set the threshold as the values of L_i that results in the lowest energy consumption but still achieves the delay and loss requirements. The process continues till the thresholds for all frequencies have been determined.

Intuitively, the proposed threshold selection scheme tries to set the thresholds in such a way that the largest possible range of queue lengths is allocated to the lowest frequency since that results in the greater energy savings. Also, for each frequency, the threshold selection scheme tries to push the threshold as close as possible to the threshold for the next higher frequency (or toward the buffer size B for frequency f_N) while still satisfying the loss and delay requirements. While the greedy approach does not necessarily result in the optimal threshold selection, it significantly reduces the search space.

V. SIMULATION RESULTS

In this section we present simulation results to evaluate the proposed mechanism for threshold selection in wireless nodes with DFS. The simulations were conducted in the NS-2 simulation platform wherein a DFS system that uses threshold based frequency selection was implemented. Our DFS mechanism has the ability to choose from a set of five operating frequencies. The five frequencies and the packet service rate (per second) associated with each frequency is shown in Table I. The energy consumed by each frequency was accounted for by implementing an energy model based on the expressions of Section II in NS2. For the implementation of the DFS mechanism, we consider the case where each node has a physical queue where the packets are stored and the DFS mechanism selects the operating frequency based on the state of this queue.

The proposed framework is evaluated under two traffic arrival processes: Poisson traffic arrivals and a 2-state Markov Modulated Poisson Process (MMPP) which are both special cases of a MAP. In our simulations, the nodes used the user datagram protocol (UDP) as the transport layer and IEEE 802.11 was used as the MAC layer. Each simulation run was for 1000 seconds and each reported value is the average of 10 runs. The length of each packet was 1000 bytes. The buffer size at each node was assumed to be $B = 50$ packets. The simulations consider a two node scenario with one access point and one subscriber station.

A. Results for Poisson Traffic

To understand the impact of the choice of various thresholds and also to validate the proposed queueing model for DFS

TABLE I
AVAILABLE CLOCK FREQUENCIES

Frequency	Service Rate
100MHz	300
150MHz	450
200MHz	600
250MHz	750
300MHz	1000

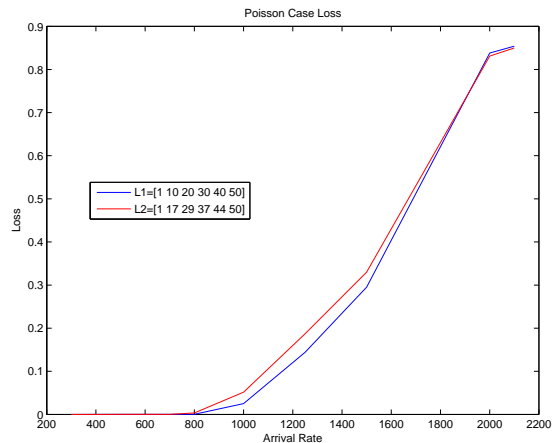


Fig. 2. Poisson Traffic: Loss Ratio

systems, we first consider the case of Poisson traffic. We consider two threshold settings: $L1 = [1, 10, 20, 30, 40, 50]$ and $L2 = [1, 17, 29, 37, 44, 50]$. Note that while $L1$ uniformly divides the range of queue lengths between the five frequencies, $L2$ uses the lowest frequency for a larger range of queue lengths.

The analytic results for the packet drop rates experienced for the two thresholding cases for various packet arrival rates is shown in Figure 2. The corresponding average energy consumption is shown in Figure 3. We note that the performance of the two threshold levels is approximately the same in terms of the packet drop rates. This is primarily because in both cases, the DFS selects the highest frequency as the queue length approaches B . However, the use of $L2$ significantly reduces the average energy consumption, specially at moderate loads. When the arrival rate (and thus the load) is very low, the queue lengths are low and both systems tend to use the lowest frequency for most of the time. At moderate loads, $L2$ gives significant energy savings compared to $L1$ because it uses lower frequencies for a larger range of queue lengths. Also, at very high arrival rates where the system is highly loaded, both thresholds have a similar performance since both operate at the highest frequency.

The loss rates from our analytic model are compared with simulation results in Table II while the results for the energy consumption are shown in Table III. We note that the results show a good match for the both the energy consumption and loss rates. The loss results predicted by the analysis is higher than that of the simulations.

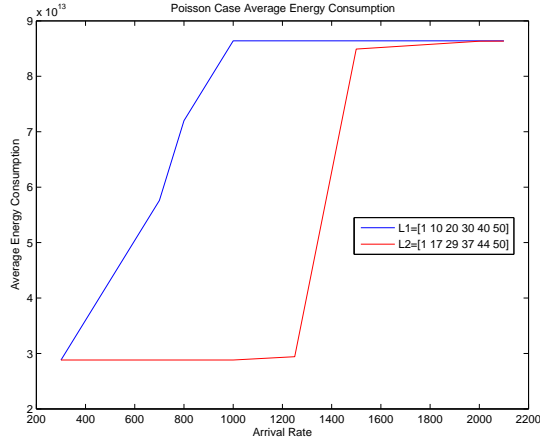


Fig. 3. Poisson Traffic: Average Energy Consumption

TABLE II
POISSON TRAFFIC: LOSS RATES

λ	$L1$		$L2$	
	Analysis	Simulation	Analysis	Simulation
300	6.92E-18	0	7.21E-17	0
500	1.27E-09	0	1.46E-13	0
700	1.81E-04	0	3.67E-06	0
800	3.47E-03	0	4.23E-04	0
1000	5.16E-02	9.36E-05	1.53E-02	0
1250	1.87E-01	2.44E-02	1.14E-01	1.07E-02

B. Results for 2-State MMPP Traffic

To evaluate the proposed model under more realistic traffic models, next we consider the case where the arrivals were generated according to a 2-state MMPP. For these results, the transition probabilities $p_{i,j}$ and $q_{i,j}$ for the C and D matrices were kept constant while the arrival rates λ_i were varied to generate traffic at different rates. The C and D matrices were:

$$C = \begin{bmatrix} -0.1 - \lambda_1 & 0.1 \\ 0.2 & -0.2 - \lambda_2 \end{bmatrix}, \quad D = \begin{bmatrix} \lambda_1 & 0 \\ 0 & \lambda_2 \end{bmatrix}$$

with $\lambda_2/\lambda_1 = 4$. For MMPP arrivals, Figures 4 and 5 show the packet drop rates and average energy consumption for the two thresholds: $L1 = [1, 10, 20, 30, 40, 50]$ and $L2 = [1, 17, 29, 37, 44, 50]$. The simulation results have accuracy similar to the Poisson case and have been omitted due to space constraints.

Compared to the Poisson case, the loss rates for the two thresholds is significantly different for MMPP arrivals. This is because the MMPP arrival process is significantly more burstier than the Poisson arrivals. As a result, $L1$ has lower loss rates since it uses the highest frequency for a larger range of queue lengths, allowing it to better absorb bursts of arrivals. The trend for the average energy consumption follow those for the Poisson case with threshold $L2$ resulting in lower energy consumption at moderate loads.

TABLE III
POISSON TRAFFIC: AVERAGE ENERGY CONSUMPTION

λ	$L1$		$L2$	
	Analysis	Simulation	Analysis	Simulation
300	2.88E+13	2.88E+13	2.88E+13	2.88E+13
500	4.32E+13	2.88E+13	4.32E+13	2.88E+13
700	5.76E+13	2.88E+13	5.76E+13	2.88E+13
800	7.20E+13	2.93E+13	7.20E+13	2.88E+13
1000	7.20E+13	2.88E+13	7.20E+13	6.30E+13
1250	7.20E+13	3.42E+13	8.64E+13	7.93E+13
1500	8.64E+13	6.02E+13	8.64E+13	8.50E+13

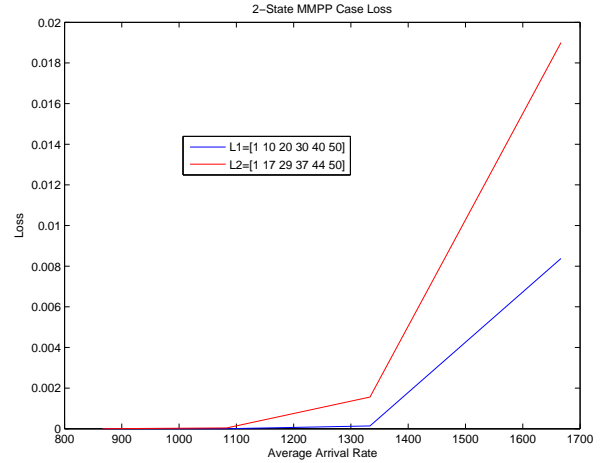


Fig. 4. MMPP Traffic: Loss Ratio

C. Optimal Threshold Selection

This section presents the results for the optimal threshold selection. Due to space constraints, we only show the results for the Poisson case and the results for MMPP arrivals show similar trends. The optimal threshold levels for Poisson traffic with different rates is shown in Table IV. We observe that as the constraint on the loss rate is made stricter, the range of queue lengths over which the lowest frequency can be used reduces. Similarly, as the arrival rate is increased, the threshold values for the frequencies moves towards lower values. Both these observations are a result of the fact that as the load increases or when lower loss rates are desired, higher frequencies need to be used to larger ranges of the queue length. We also note that energy consumed increases as the load increases. This is because at higher loads the system operates at higher frequencies for a greater fraction of time, leading to higher energy consumption.

VI. CONCLUSIONS

This paper presented a methodology for the optimal selection of thresholding frequencies for wireless network hardware equipped with DFS. The proposed framework is based on modeling each node as a $MAP/G/1/K$ queue with threshold based service. Our simulation results show that the proposed

TABLE IV
POISSON TRAFFIC:OPTIMAL THRESHOLD SELECTION

λ		Loss Upper Bound		
		0.01	0.02	0.03
300	Thresholds	[1 47 47 48 49 50]	[1 47 47 48 49 50]	[1 47 47 48 49 50]
	Energy	2.88E+13	2.88E+13	2.88E+13
	Loss	5.71E-08	5.71E-08	5.71E-08
600	Thresholds	[1 38 41 48 49 50]	[1 25 44 48 49 50]	[1 28 47 48 49 50]
	Energy	5.76E+13	4.32E+13	4.32E+13
	Loss	9.94E-03	1.99E-02	2.93E-02
900	Thresholds	[1 22 23 25 49 50]	[1 32 32 34 49 50]	[1 33 34 38 49 50]
	Energy	7.20E+13	7.20E+13	7.20E+13
	Loss	9.94E-03	0.019963419	0.029833535

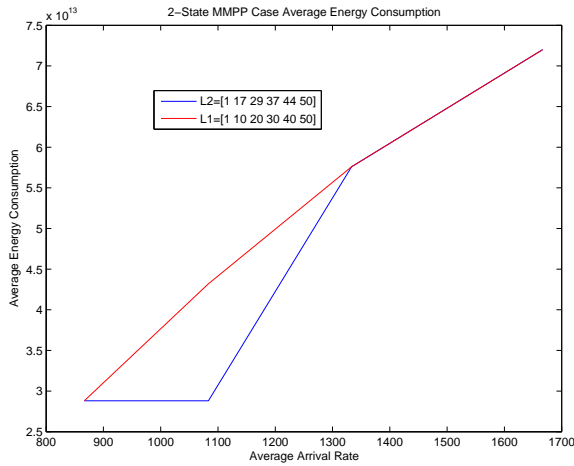


Fig. 5. MMPP Traffic: Average Energy Consumption

scheme achieves the minimum energy consumption while ensuring that packet level performance characteristics are maintained.

APPENDIX

The quantities x used in the model presented in Section III represent the system state at the departure epochs. Let τ_k , $k \geq 1$, denote the epochs of successive departures with $\tau_0 = 0$. Also, we denote the queue length and state of the Markov arrival process immediately after the k -th departure as Q_k and J_k , respectively. The probabilities $x_{i,j}$ and the vector x are then defined as

$$x_{i,j} = \lim_{k \rightarrow \infty} Pr\{Q_k = i, J_k = j\}, \quad 0 \leq i \leq B-1, 1 \leq j \leq m$$

$$x_i = (x_{i,1}, x_{i,2}, \dots, x_{i,m}),$$

$$x = (x_0, x_1, \dots, x_{B-1}).$$

The matrices A_k^r form the one-step transition probabilities of the Markov chain $\{(Q_k, J_k)\}$. The matrix A_k^r is given by

$$A_k^r = \int_0^\infty P(k, x) dG_{S,r}(x), \quad 1 \leq j \leq N, k \geq 0 \quad (14)$$

where $G_{S,r}(x)$ is the cumulative distribution function of the service time when frequency r , $1 \leq r \leq N$, is chosen. Also, the (i, j) -th element of the $m \times m$ matrix $P(k, x)$ is defined as the conditional probability

$$p_{i,j}(k, x) = Pr\{M(x) = k, J(x) = j \mid M(0) = 0, J(0) = i\},$$

$$k \geq 0, 1 \leq i, j \leq m \quad (15)$$

where $M(x)$ is the number of packet arrivals in the interval $(0, x]$. Finally, $E = x_0(-C^{-1})e + s_1 x_0 e + \sum_{k=1}^N s_k \sum_{n=L_{k-1}}^{L_k-1} x_n e$ is the mean time between two successive departures from the queue.

REFERENCES

- [1] B. Sikdar, "A study of the environmental impact of wired and wireless local area network access," *IEEE Transactions on Consumer Electronics*, vol. 59, no. 1, February 2013.
- [2] O. Arnold, F. Richter, G. Fettweis and O. Blume, "Power consumption modeling of different base station types in heterogeneous cellular networks," *Proceedings of Future Network and Mobile Summit*, Florence, Italy, June 2010.
- [3] H-S. Jung, A. Hwang and M. Pedram, "Predictive-flow-queue based energy optimization for gigabit Ethernet controllers," *IEEE Transactions on VLSI Systems*, vol. 17, no. 8, pp. 1113-1126, August 2009.
- [4] J. Chen and B. Sikdar, "A Mechanism for Load Proportional Energy Use in Wireless Local Area Networks," *Proceedings of IEEE GLOBECOM*, Atlanta, GA, December 2013.
- [5] K. Choi, R. Soma and M. Pedram, "Dynamic voltage and frequency scaling based on workload decomposition," *Proceedings of Symposium on Low Power Electronics and Design*, pp. 174-179, Newport Beach, CA, August 2004.
- [6] R. Bolla, R. Bruschi and C. Lombardo, "Dynamic Voltage and Frequency Scaling in Parallel Network Processors," *Proceedings of IEEE HPSR*, pp. 242-249, Belgrade, Serbia, June 2012.
- [7] S. Shah-Heydari and T. Le-Ngoc, "MMPP models for multimedia traffic," *Telecom. Sys.*, vol. 15, no. 3-4, pp. 273-293, Dec 2000.
- [8] A. Andersen and B. Nielsen, "A Markovian approach for modeling packet traffic with long range dependence," *IEEE Journal on Selected Areas in Communications*, vol. 16, no. 5, pp. 719-732, June 1998.
- [9] G. Bianchi, "Performance analysis of the IEEE 802.11 distributed coordination function," *IEEE Journal on Selected Areas in Communications*, vol. 18, no. 3, pp. 535-547, March 2000.
- [10] D. Choi, "MAP/G/1/K Queue with Multiple Thresholds on Buffer," *Comm. Korean Math. Society*, vol. 14, no. 3, pp. 611-625, 1999.